

## Scientific-Research Article

# Dynamic stiffness matrix for analysis of modal properties the damaged composite wing

Shahrokh Shams<sup>1\*</sup>, A.R. Torabi<sup>2</sup>, Mahdi Fatehi Narab<sup>3</sup>

1-3- Department of Aerospace Engineering, Faculty of New Sciences and Technologies, University of Tehran

2-Fracture Research Laboratory, Faculty of New Science and Technologies, University of Tehran

\* North Kargar Street, Tehran, Iran

Email: \* sh\_shams56@yahoo.com

*In this paper, damage in composite wings is introduced, firstly, then using Euler-Bernoulli equations with including flexural and torsional coupling, governing equations on cantilevered composite wing is derived. By applying separation method damaged beam is converted to two interconnected intact beams and using boundary conditions and continues conditions in damage location, the dynamic stiffness matrix is composed and modal analysis of damaged wing is done. Composite type is fiber-reinforced and damage type is edge crack with various locations and depths. Also effects crack depths and locations on modal properties in various fiber angle are examined. Results showed that existence a crack even with small depth in root of large span wing can reduce natural frequencies, seriously.*

**Keywords:** “Cracked wing”, “Dynamic stiffness matrix”, “Modal properties”, “interconnected beam”

## Introduction

Inherent flaws from the manufacturing processes as well as design deficiencies may account for the original sources of the wing failure; internal damage such as delamination, fiber/matrix cracking and de-bonding between matrix and fibers could be the direct outcome of impact and/or fatigue loading during the flight [1]. The modal analysis in damaged composite structure is very important because of damage leading to reduction of stiffness

and as a result of it natural frequency is decreased, and structure under the influence of damage can be failure. On the other hand basic analysis and prerequisite for many of other analysis such as SHM and aero-elastic is modal analysis [2]. In this study modal analysis cracked composite wing is considered. Wing is modeled as cantilevered beam and damaged beam is modeled as two interconnected intact beam. Boundary conditions in fixed and free ends, continues conditions in crack location and dynamic stiffness matrix method is

---

1 Assistant professor (corresponding author)

2 Associate Professor

3 PhD Student

used for modal analysis. Two case study for high and low aspect ratio wing is studied. Results showed that in damaged wing with crack location in root and case study large span, natural frequency is reduced, severely.

## Theory

### The governing equations

In the figure 1 cracked composite wing model is showed in which wing span, wing chord, layer thickness, crack location and crack depth are demonstrated with  $L$ ,  $b$ ,  $t$ ,  $l$  and  $a$ , respectively. Also principle axes and fiber angle are showed with (1,2) and, respectively

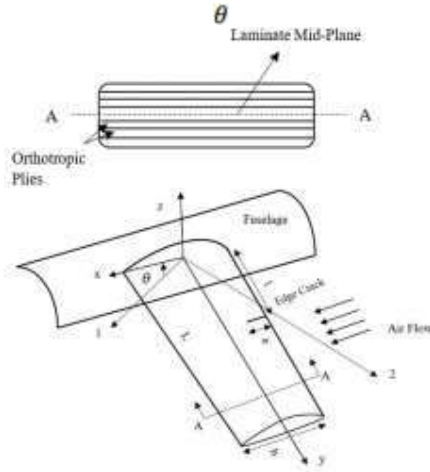


**Fig1:** The co-ordinate system and notation for a bending-torsion coupled composite wing bending-torsion coupled composite wing

For extracting of governing equations on composite wing, Euler-Bernoli beam model including Lottati [3] method is used.

$$\begin{cases} EI \frac{d^2}{dy^2} \left( \frac{d^2 h}{dy^2} \right) + K \frac{d}{dy} \left( \frac{d^2 \psi}{dy^2} \right) + m \frac{d^2 h}{dt^2} - m x_\alpha \frac{d^2 \psi}{dt^2} = 0 \\ GJ \frac{d^2 \psi}{dy^2} + K \frac{d}{dy} \left( \frac{d^2 h}{dy^2} \right) + m x_\alpha \frac{d^2 h}{dt^2} - I_\alpha \frac{d^2 \psi}{dt^2} = 0 \end{cases} \quad (1)$$

Where,  $h(y,t)$  is the bending displacement of a point on the elastic axis and  $\psi(y,t)$  is the torsional rotation about the elastic axis,  $EI = EI(y)$  and  $GJ = GJ(y)$  are the bending and torsional stiffnesses, respectively. Mass moment of inertia about the elastic axis is denoted by  $I_\alpha$  and  $x_\alpha$  is the distance between the inertia axis and the elastic axis [4].

Assuming harmonic oscillation for bending and torsion motion and using the separation of variables method, general solution in the normalized coordinate  $\xi$  for bending and torsion deflection is achieved:

$$h(y,t) = H(\xi)e^{i\omega t}, \psi(y,t) = \Psi(\xi)e^{i\omega t} \quad (2)$$

Then expressions for the cross-sectional rotation, the bending moment, the shear force and the torsional moment for the cantilevered beam are obtained

$$\Theta(\xi) = \frac{1}{L} \frac{dH(\xi)}{d\xi} \quad (4)$$

$$S(\xi) = \frac{EI}{L} \frac{d^3 H(\xi)}{d\xi^3} + \frac{K}{L^2} \frac{d^2 \Psi(\xi)}{d\xi^2} \quad (5)$$

$$M(\xi) = -\frac{EI}{L^2} \frac{d^2 H(\xi)}{d\xi^2} - \frac{K}{L} \frac{d\Psi(\xi)}{d\xi} \quad (6)$$

$$T(\xi) = -\frac{K}{L^2} \frac{d^2 H(\xi)}{d\xi^2} - \frac{GJ}{L} \frac{d\Psi(\xi)}{d\xi} \quad (7)$$

Using the boundary conditions in fixed and free ends, continues boundary in crack location, stiffness matrix, similar to Banerjee [5] is achieved.

at the fixed end,  $\xi = 0$

$$H(0) = \Theta(0) = \Psi(0) = 0 \quad (8)$$

at the free end,  $\xi = 1$

$$M(1) = S(1) = T(1) = 0 \quad (9)$$

Cracked beam modeling, similar to Wang [6], is done by two interconnected intact beam

$$\begin{aligned} 0 \leq \xi \leq \xi_c \rightarrow H_1(\xi) &= A_1 \cosh \alpha \xi + A_2 \sinh \alpha \xi - A_4 \sin \beta \xi + A_5 \cos \gamma \xi + A_6 \sin \gamma \xi \\ \Psi_1(\xi) &= B_1 \cosh \alpha \xi + B_2 \sinh \alpha \xi + B_3 \cos \gamma \xi + B_4 \sin \beta \xi + B_5 \cos \gamma \xi + B_6 \sin \gamma \xi \\ \xi_c \leq \xi \leq 1 \rightarrow H_2(\xi) &= A_7 \cosh \alpha \xi + A_8 \sinh \alpha \xi + A_9 \cos \beta \xi + A_{10} \sin \beta \xi + A_{11} \cos \gamma \xi + A_{12} \sin \gamma \xi \\ \Psi_2(\xi) &= B_7 \cosh \alpha \xi + B_8 \sinh \alpha \xi + B_9 \cos \beta \xi + B_{10} \sin \beta \xi + B_{11} \cos \gamma \xi + B_{12} \sin \gamma \xi \end{aligned} \quad (10)$$

The additional boundary conditions or continues boundary conditions in crack location are:

$$\begin{aligned} M_1(\xi_c) &= M_2(\xi_c), \\ S_1(\xi_c) &= S_2(\xi_c), T_1(\xi_c) = T_2(\xi_c) \\ H_2(\xi_c) &= H_1(\xi_c) + c_{22}S_1(\xi_c) + c_{26}T_1(\xi_c) \\ \Theta_2(\xi_c) &= \Theta_1(\xi_c) + c_{44}M_1(\xi_c) \\ \Psi_2(\xi_c) &= \Psi_1(\xi_c) + c_{62}S_1(\xi_c) + c_{66}T_1(\xi_c) \end{aligned} \quad (11)$$

$c_{ij}$  are coefficients of local flexibility matrix.

From Eqs.(11) and equations related to boundary conditions, dynamic stiffness matrix will be yielded.

$$[\Lambda]_{12 \times 12} [A]_{12 \times 1} = [0]_{12 \times 1} \quad (12)$$

The natural frequencies are equal to frequencies that lead to zeroing coefficients matrix (dynamic stiffness matrix) determinant ( $[\Lambda] = 0$ ).

### Case studies

To verifying of results, the intact wing model from Ref. [1] is selected, firstly. The model geometry of the cantilever wing is taken to be: length  $L = 1.0$  m, width  $b = 0.25$  m, thickness  $t = 0.02$  m and offset of the center of gravity  $S = 0.05$  m. Fig 2 illustrates the variation of bending stiffness parameter ( $EI$ ), torsional stiffness parameter ( $GJ$ ), coupling parameter ( $K$ ) and  $\Psi (= \frac{K}{\sqrt{EI \cdot GJ}})$  for fiber angles between  $0^\circ$  and  $180^\circ$ . Fig 2 indicates the symmetry of  $EI$  and  $GJ$  and anti-symmetry of  $K$  and  $\Psi$  with respect to the fiber angle. Fig3 shows the variation of the first four natural frequencies for the same range of fiber angles. This figure indicates the symmetric nature of natural frequencies for beams without the inertia coupling ( $S=0$ ).

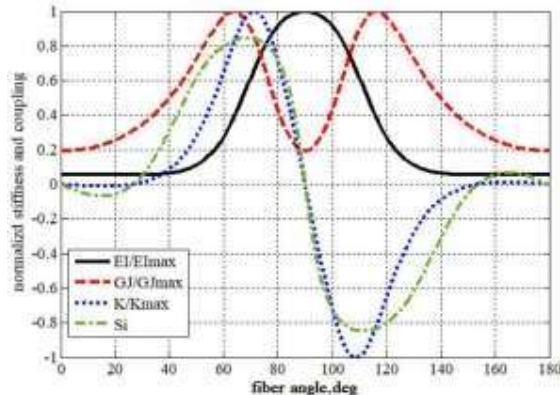


**Fig 2:** Variation of the elastic parameters  $EI$ ,  $GJ$ ,  $K$  and  $\Psi$  with respect to fiber angles

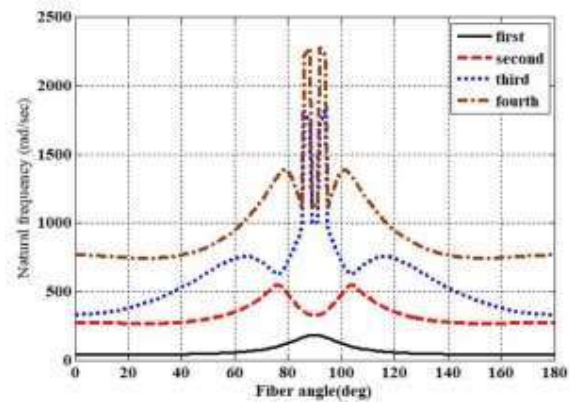


**Fig3:** Variation of the first four natural frequencies with respect to fiber angles (without inertia coupling:  $S=0$ )

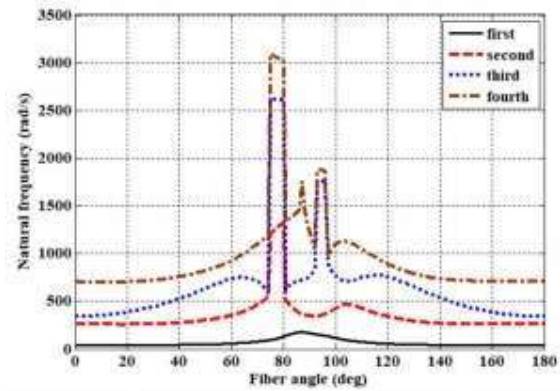


**Fig4:** Variation of the first four natural frequencies with respect to fiber angles (with inertia coupling:  $S=0.05$ )

Except for the first natural frequency as shown in Fig4, the symmetric nature of natural frequencies for beams without the inertia coupling no longer exists for the wing model including the inertia coupling. And in order to determine of crack effects on vibration analysis, two case study are investigated. Case study I related to unidirectional composite beam consists of several plies aligned in the same direction. Material and geometric properties of beam have given in Table 1.

**Table 1:** Properties of case study I of cracked wing

Modulus of elasticity-matrix	$E_m = 2.76$ GPa
Modulus of elasticity-fiber	$E_f = 275.6$ GPa
Modulus of rigidity-matrix	$G_m = 1.036$ GPa
Modulus of rigidity-fiber	$G_f = 114.8$ GPa
Mass density of matrix	$\rho_m = 1600$ kg/m <sup>3</sup>
Mass density of fiber	$\rho_f = 1900$ kg/m <sup>3</sup>
Length	$L = 0.5$ m
Width	$b = 0.1$ m
Thickness	$t = 0.005$ m
Fiber angle	$\theta = 30^\circ, 70^\circ$
Offset of the center of gravity	$S = 0$

The first natural frequency variations with respect to crack location (at the fiber angle 35deg and crack depth ratio 0.3) shown that lowest of the first natural frequency has happened when crack location is at root and highest frequency has happened when crack location is at tip. Thus, whatever the crack's location farther away from wing root, the first natural frequency is higher and wing structure is more safe (Fig 5).

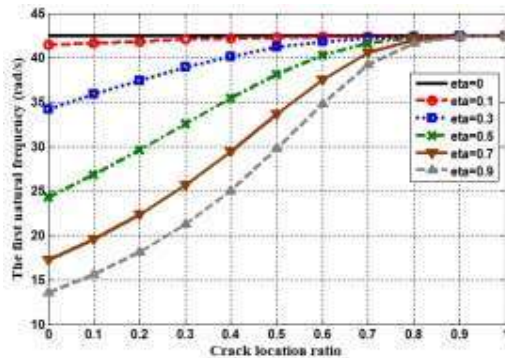


**Fig 5:** The first natural frequency changes w.r.t crack locations in various crack depths (eta) for case study I with the properties given in table 1 at fiber angle 30deg.

The first natural frequency variations with respect to fiber angle (at crack location in root and various and various crack depth ratios) shown that lowest of the first natural frequency has happened when crack depth ratio is 0.6 and fiber angle is at maximum coupling (70 deg) on the other hand in this crack depth ratio maximum natural frequency has happened at minimum coupling (90 deg).

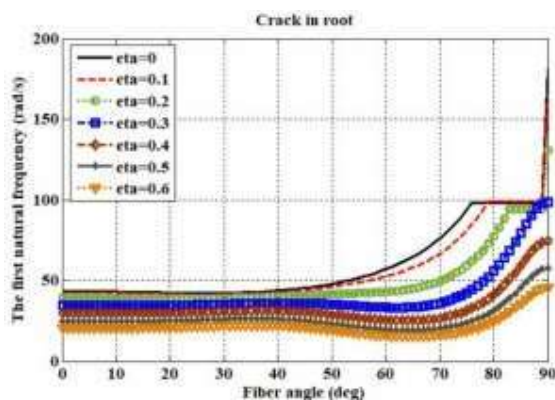


**Fig 6:** The first natural frequency changes w.r.t fibre angles in various crack depths (eta) for case study I with the properties given in table 1.

In following, edge crack effects on high aspect ratio composite Goland wing with properties given in Table 2 will be investigated. The Goland wing

model used in this work is based on the described model in Ref [5].

**Table 2.** Properties of case study II of cracked wing

Bending rigidity	$EI = 9.75 \times 10^6 N.m^2$
Torsional rigidity	$GJ = 9.88 \times 10^5 N.m^2$
bending-torsion coupling rigidity	$K = 0.1, 1.5, 2.2, 2.5 \times 10^6 N.m^2$
mass per unit length	$m = 35.75 kg/m$
mass moment of inertia per unit length	$I_a = 8.65 kg.m$
distance between the mass and elastic axes	$x_a = 0.0, 0.1, 0.2, 0.3 m$
Length	$L = 6 m$
Width	$b = 1.83 m$

In Fig 7 and Fig 8 upward behavior of the first natural frequency in bending and torsion mode for crack location from root to tip has been plotted. It is showed that by moving the crack from root to tip, the first natural frequency is increased.

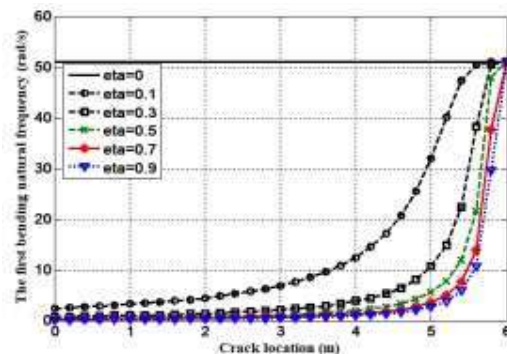


**Fig 7:** The bending natural frequency changes w.r.t crack locations in various crack depths (eta) for Goland wing.

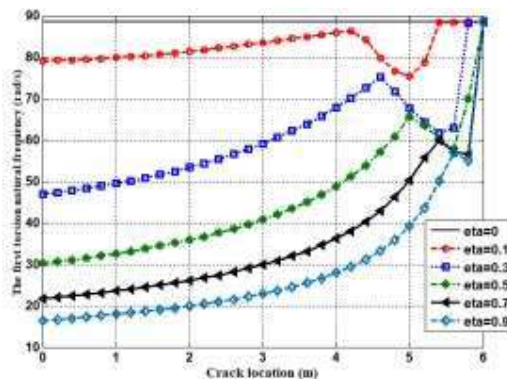


**Fig 8:** The torsion natural frequency changes w.r.t crack locations in various crack depths (eta) for Goland wing.

## Results and discussion

In this paper showed the symmetry of variation of bending stiffness parameter (EI), torsional stiffness

parameter (GJ) and anti-symmetry of coupling parameter (K) and  $\Psi$  with respect to the fiber angle. Also showed that inertia coupling (the distance between the mass and elastic axes) leading to, except for the first natural frequency, anti-symmetry behavior of natural frequencies. In following showed that edge crack in composite wing reduces the stiffness of system and as a result of it the natural frequency is decreased. As explained, the amount of this decrease depends on the crack depth, crack location and fiber angle. As crack depth increases and crack distance from root of wing decreases, the effect of the crack on the decrease of the natural frequency increases so that for  $\eta=0.5$  and crack location in root, in case study I, the decrease of the natural frequency 25 rad/sec from 42.35 is obtained. Based on the results in case study II, decrease of the natural frequency is more intensive because wing span is high.

### Conclusions

After studying variations of geometric and material coupling with respect to fiber angle and reviewing the results of cracked composite wing in two case I and II, it concluded that the amount of decrease of the natural frequency due to of edge crack depends on the crack depth, crack location fiber angle and span of wing. The results showed the crack (even with shallow depth) in root of large span wing decreases the natural frequency, severely. Therefore structural designers should use from different methods such as aero-elastic tailoring and SHM to reduce this danger.

### References

- [1] K. Wang, "Vibration Analysis of Cracked Composite Bending-torsion Beams for Damage Diagnosis," Virginia Polytechnic Institute and State University, 2004.
- [2] Y. Kim, T. Strganac and A. Kurdila, "Nonlinear flutter of composite plates with damage evolution," in *34th Structures, Structural Dynamics and Materials Conference*, 1993.
- [3] I. Lottati, "Flutter and Divergence Aeroelastic Characteristics for Composite Forward Swept Cantilevered Wing," *AIRCRAFT*, pp. 1001-1007, 1985.
- [4] L. Meirovitch and L. Silverberg, "Active vibration suppression of a cantilever wing," *Journal of Sound and Vibration*, vol. 97(3), pp. 489-498, 1984.
- [5] J. R. Banerjee, H. Su and C. Jayatunga, "A dynamic stiffness element for free vibration analysis of composite beams and its application to aircraft wings," *Computers and Structures*, vol. 86, pp. 573-579, 2008.
- [6] K. Wang, D. Inman and C. Farrar, "Crack-induced Changes in Divergence and Flutter of Cantilevered Composite Panels," *Journal of Structure Health Monitoring*, vol. 4(4), pp. 377-392, 2005.
- [7] K. Wang, *Vibration Analysis of Cracked Composite Bending-torsion Beams for Damage Diagnosis*, Blacksburg, Virginia: Virginia Polytechnic Institute and State University, November 29, 2004.
- [8] L. Meirovitch and I. Tuzcu, "Unified theory for the dynamics and control of maneuvering flexible aircraft," *AIAA*, vol. 42, no. 4, p. 714-727, 2004.